Apparent impedance analysis: A new method for power system stability analysis

Atle Rygg, Mohammad Amin and Marta Molinas
Department of Engineering Cybernetics
Norwegian University of Science and Technology
Trondheim, Norway
Email: atle.rygg@ntnu.no

Bjørn Gustavsen
SINTEF Energy Research
Trondheim, Norway

***Abstract*—In this paper a new method for power system stability analysis is introduced. The method is based on injection of a small voltage or current in an arbitrary point of the system. The apparent impedance is defined as the ratio between the voltage and current in the injection point. It is shown that the apparent impedance can be used to estimate the eigenvalues of the system that are observable from the injection point. The eigenvalues are obtained by applying the Vector Fitting algorithm to the measured set of apparent impedances. The proposed method holds some advantages over the well established impedance-based analysis method: It is no longer needed to estimate the source and load impedance equivalents separately, and it is not necessary to make any assumption regarding where the source and load are located. This reduces the required measurements and data processing. Furthermore, the stability analysis is global in the sense that the resulting stability margin does not depend on the injection point location. Finally, the method is well suited for real-time implementation due to low computational requirements. The method is outlined for DC-systems, while further work will extend the theory to cover single-phase and three-phase AC systems.**

***Index Terms*—Vector Fitting, State-space modeling, Impedance-based analysis, Power system stability analysis.**

I. Introduction

Stability analysis of power systems is often conducted by small-signal methods. Two branches of small-signal methods exist: impedance-based analysis and state-space analysis. The advantage of state-space analysis is the ability to decompose system dynamics into different oscillation modes, and to assess the stability of each mode by eigenvalues and participation factors. The main drawback of state-space analysis is that detailed information and parameter values for all units in the system are usually required. The impedance-based method is an alternative method which decomposes the system into a source and load impedance equivalent [1], [2], [3]. Stability can be analyzed by applying the Nyquist Criterion to the ratio between source and load impedance. The main advantage of the impedance-based method is that stability can be analyzed from measurement/simulations in a single point in the system. Hence, this can be viewed as a black-box approach. In order to perform such analysis, a disturbance or perturbation must normally be injected into the system. The impedance-based analysis has traditionally been applied to power systems based on power electronic converters.

This paper proposes a new method for stability analysis called the apparent impedance method. The approach is based on measurements in a single point similar to the above mentioned impedance-based analysis. But instead of applying the Nyquist Criterion, the method identifies the system eigenvalues based on the measured impedance values. Furthermore, it is not required to estimate the source and load impedances separately. Only the apparent impedance as defined in (1) needs to be estimated. A major advantage with the apparent impedance method is that the resulting stability estimate does not depend on the measurement location and therefore provides a global stability margin. Finally, the number of measurements required for stability analysis is lower than the traditional impedance-based analysis.

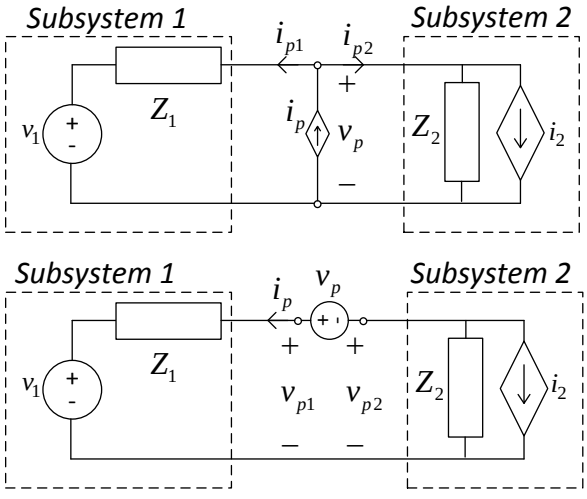

Fig. 1: General DC power system partioned into two subsystem with shunt or series injection

II. Apparent impedance definition

The definition of the apparent impedance assumes an injection of voltage or current at some point in the system. In Fig. 1 an injection is applied to a DC system composed by two subsystems. The injection point separates the system into two subsystems (1 and 2), here represented by their frequency-dependent Thevenin and Norton equivalents. It will be shown later that the choice of Thevenin vs. Norton does not impact the stability analysis. The upper part of Fig. 1 represent shunt injection, while the lower part represent series injection. The choice of shunt vs. series injection has an impact on the methodology as illustrated in Fig 2.

The apparent impedance is defined as:

$$Z_a(s) = \frac{v_p(s)}{i_p(s)} = \frac{1}{Y_a(s)} \tag{1}$$

where v_p and i_p are defined in Fig. 1. The apparent admittance $Y_a(s)$ is defined as the inverse of the apparent impedance. The relation between Z_a and the subsystem impedances Z_1 and Z_2 depends on the choice of shunt vs. series injection. When deriving these expressions we can neglect the impact from the sources v_1 and i_2 due to the small-signal assumption. The following expressions can then be obtained for Z_a by circuit analysis applied to Fig. 1:

$$Z_{a,shunt} = Z_1 || Z_2 = \frac{Z_1 Z_2}{Z_1 + Z_2} \tag{2}$$

$$Z_{a,series} = Z_1 + Z_2 = \frac{Y_1 Y_2}{Y_1 + Y_2} \tag{3}$$

Note that these expressions do not depend on the type of subsystem equivalent (Thevenin vs. Norton) since we are disregading the impact of the voltage and current sources during small-signal analysis. The application of apparent impedance in stability analysis is explained in the next section.

III. Stability analysis by the apparent impedance

Apparent impedance stability analysis is a small signal method. The objective is to estimate all eigenvalues of the system based on sampled values of Z_a. The stability analysis follows directly by evaluating the eigenvalues in the complex plane. A flowchart of the methodology is presented in Fig. 2:

A. State-space modeling and transfer functions

In small-signal analysis it is assumed that the entire system can be represented by a linear state-space model:

$$\begin{aligned} s\underline{x} &= A\underline{x} + Bu \\ y &= C\underline{x} + (D + sE)u \end{aligned} \tag{4}$$

where $\underline{x}$ is the vector of n *states*, u is the single input to the system, while y is the single output. A is the $n \times n$ state matrix, B is a $n \times 1$-vector, C is a $1 \times n$-vector, while D and E are scalars. Note that (4) assumes a Single-Input-Single-Output (SISO) system, which is the case for a DC-system.

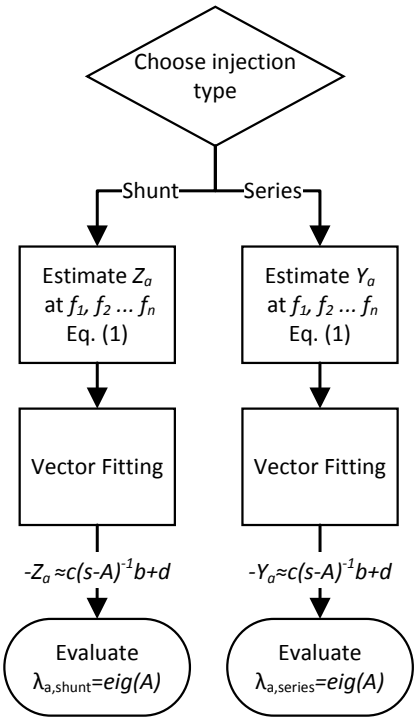

Fig. 2: Flowchart of apparent impedance stability analysis

In case of three-phase systems, u, y, D, E would also become vectors, while B would become a matrix.

By control theory, an impedance represents a transfer function between current and voltage. With reference to the state-space model (4), a general transfer function $H(s)$ can be defined as the ratio between output y and input u:

$$H(s) = \frac{y(s)}{u(s)} = C\left(sI - A\right)^{-1} B + D + sE \tag{5}$$

A general impedance $Z(s)$ and admittance $Y(s)$ can be defined accordingly based on some voltage v and some current i.

$$\begin{aligned} Z(s) &= \frac{v(s)}{i(s)} = C_Z\left(sI - A_Z\right)^{-1} B_Z + D_Z + sE_Z \\ Y(s) &= \frac{i(s)}{v(s)} = C_Y\left(sI - A_Y\right)^{-1} B_Y + D_Y + sE_Y \end{aligned} \tag{6}$$

For the following analysis the circuit diagrams in Fig. 1 have been transformed to block diagrams in Fig. 3.

For a moment it is assumed the injection sources do not exist. For shunt current injection, the transfer function between subsystem 2 load current i_2 and the interface point voltage v_p is then expressed as:

$$\frac{v_p(s)}{i_2(s)} = -\frac{Z_1 Z_2}{Z_1 + Z_2} = -Z_{a,shunt} \tag{7}$$

where the last equality is obtained from (2). Similarly under series voltage injection, the transfer function between

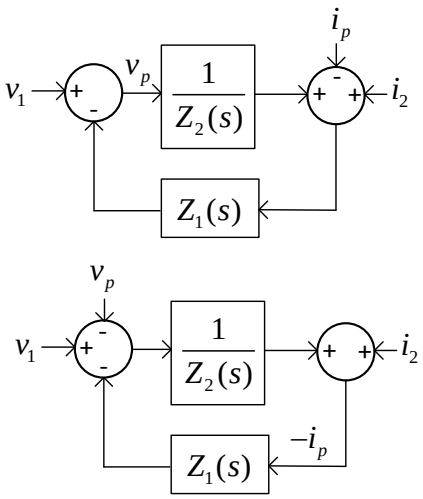

Fig. 3: Block diagram of the circuit in Fig. 1. Upper figure: shunt injection, lower figure: series injection

subsystem 1 source voltage v_1 and interface point current i_p is expressed as:

$$\frac{i_p(s)}{v_1(s)} = -\frac{1}{Z_1 + Z_2} = -\frac{1}{Z_{a,series}} = -Y_{a,series} \tag{8}$$

where the last equality is obtained from (3). This is the key point in the deriving process: the apparent impedance represents a closed-loop transfer function in the system both for shunt and for series injection. Note that the negative sign will not influence the stability analysis.

The next step in deriving the apparent impedance method is to rewrite the general transfer function in (5) according to the inputs and outputs in (7) and (8):

$$\begin{aligned} -Z_{a,shunt}(s) &= \frac{v_p(s)}{i_2(s)} \\ &= C_Z \left(sI - A_Z\right)^{-1} B_Z + D_Z + sE_Z \end{aligned} \tag{9}$$

$$\begin{aligned} -Y_{a,series}(s) &= \frac{i_p(s)}{v_1(s)} \\ &= C_Y \left(sI - A_Y\right)^{-1} B_Y + D_Y + sE_Y \end{aligned} \tag{10}$$

The matrices A_Z and A_Y will contain the system eigenvalues that are observable from the injection point. The final step in the method is to estimate the state-space models in (9) and (10) based on a set of measured/simulated values of Z_a. The system eigenvalues can then be computed and the stability analysis is complete. The Vector Fitting (VF) method is applied for this purpose in the next section.

B. Estimating state-space model by the Vector Fitting method

Vector Fitting (VF) is a well established method for rational approximation in the frequency domain using poles and residues [4] [5] [6]. The method is able to estimate a state-space model to a measured or computed transfer function based on curve fitting. Vector Fitting is widely applied in many engineering fields, from high-voltage power systems to microwave systems and high-speed electronics. A Matlab-implementation of the method is available online [7].

The input to the vector fitting algorithm is:

- A set of measured/simulated apparent impedance values function values $Z_{a1}, Z_{a2}...Z_{an}$ taken at the frequencies $f_1, f_2...f_n$ (convert to Y_a for series voltage injection).
- The order of the resulting state-space model. The maximum possible value is the number of impedance values (n).

The output of VF is then the state-space model represented by A, B, C, D, E (4). For convenience, the matrix A is represented on diagonal form, hence the eigenvalues are directly available on its diagonal.

IV. Stability analysis by the Nyquist Criterion

As discussed in the introduction, the traditional impedance-based stability analysis is conducted by means of the Nyquist Criterion. The Nyquist Criterion is based on the open-loop gain of the system (also called the minor-loop gain), i.e. the product of all transfer functions in the loop. By considering the block diagram in Fig. 3, the open loop gain L is found as:

$$L(s) = \frac{Z_1(s)}{Z_2(s)} \tag{11}$$

A common assumption in impedance-based analysis is to require a stable source when unloaded, and a stable load when connected to an ideal grid [3]. In this case the Nyquist Criterion states that the system is stable if and only if $L(s)$ does not encircle the point $(-1, 0)$ when drawn in the complex plane.

While $L(s)$ represents the open-loop gain in the system, the apparent impedance represents closed-loop transfer functions as derived in (7) and (8). Comparisons between stability analysis conducted with the Nyquist Criterion and by the apparent impedance method will be presented in the simulation section.

V. Simulation results

A case study has been defined in Fig. 4. This is a DC-system where a Constant Power Load (CPL) to the right is fed by a Buck converter. The CPL consumes constant power P^* by drawing a current I_L that is inverse proportional to its terminal voltage v_{C2}. The CPL dynamics are represented by the filter time constant τ used to lowpass-filter the measured voltage v_{C2}. The Buck converter has a constant duty cycle D, switching frequency f_{sw} and an output filter represented by R_1, L_1, C_1, R_{c1}. Series impedance R_2, R_3, L_3 separates the source and load from each other. Note that the model is non-linear due to the term $i_L = \frac{P^*}{v_{C2}^2}$.

The system is represented in *MATLAB Simulink Simscape Power Systems* using a switched (detailed) model. The simulation time step is fixed and equal to $T_{sim} = 1\ \mu s$.

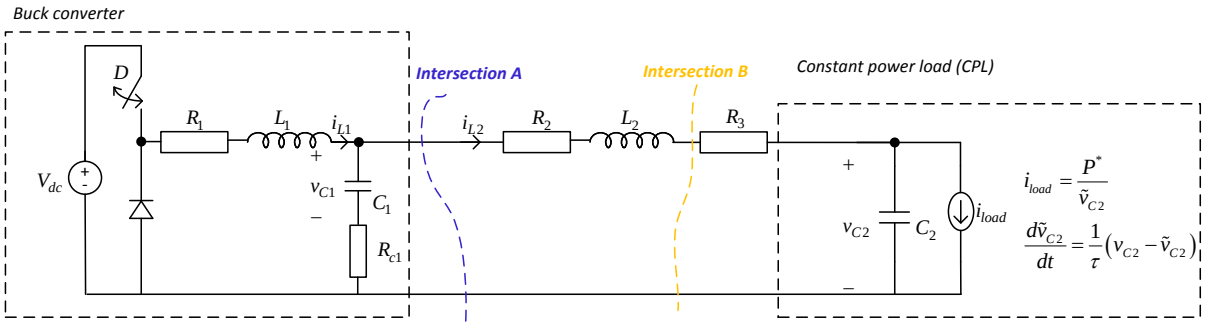

Fig. 4: Schematic of case study system

A. Analytical state-space model

By circuit analysis the state-space model of the system in Fig. 4 is derived in (12) - (13). The CPL has been linearized around its operation point denoted by the stationary voltage V_{C2}. The applied parameter values are given in Table I.

$$s \begin{bmatrix} i_{L1} \\ v_{C1} \\ i_{L2} \\ v_{C2} \\ \tilde{v_{C2}} \end{bmatrix} = A \begin{bmatrix} i_{L1} \\ v_{C1} \\ i_{L2} \\ v_{C2} \\ \tilde{v_{C2}} \end{bmatrix} \tag{12}$$

where

$$A = \begin{bmatrix} -\frac{R_1+R_{c1}}{L_1} & -\frac{1}{L_1} & \frac{R_{c1}}{L_1} & 0 & 0 \\ \frac{1}{C_1} & 0 & -\frac{1}{C_1} & 0 & 0 \\ \frac{R_{c1}}{L_2} & \frac{1}{L} & -\frac{R_1+R_2+R_{c1}}{L_2} & -\frac{1}{L_2} & 0 \\ 0 & 0 & \frac{1}{C_2} & 0 & \frac{P^*}{C_2 V_{C2}^2} \\ 0 & 0 & 0 & \frac{1}{\tau} & -\frac{1}{\tau} \end{bmatrix} \tag{13}$$

TABLE I: Parameter data applied in the simulation model

Parameter	Value	Parameter	Value
V_{DC}	2 V	D	0.5
R_1	10 $m\Omega$	L_1	0.9 mH
C_1	1.1 mF	R_{c1}	500 $m\Omega$
R_2	50 $m\Omega$	R_3	20 $m\Omega$
L_2	1.6 mH	C_2	10 mF
P^*	0.5 W	τ	5 ms.
T_{sim}	1 μs	f_{sw}	2.5 kHz

The eigenvalues $\lambda_{analytic}$ of the state matrix A have been calculated in MATLAB using the data in Table I. They are compared with the eigenvalues obtained by the proposed method in Section V-C.

B. Obtaining apparent impedances by simulation

Obtaining impedance values by simulation can be achieved by most time-domain analysis tools. The idea is to inject a small disturbance in the interface point as illustrated in Fig 1. The disturbance can contain a single frequency (single-tone), or be composed by several frequencies (multi-tone). In case of single-tone, a set of consecutive simulations must be performed in order to establish the impedance curves.

In this work, a multi-tone signal composed by 8 frequencies is injected. The frequencies are logarithmically spaced in the range between 2 and 2000 Hz as:

$$f_{inj} = [2, 6, 14, 38, 104, 278, 746, 2000]\ Hz \tag{14}$$

A time-domain simulation of steady-state operation is presented in Fig 5. Shunt current injection is applied to intersection B, and the injected current i_p as well as the intersection point voltage v_p is presented in the plot. The amplitude of each injected frequency component is 0.5 mA, giving a total RMS of $\frac{1}{\sqrt{2}} \cdot 8 = 2.8\ mA$. This is approximately 0.5 % of the average load current.

The curves in Fig. 5 is the *only* information needed to perform the remaining part of the stability analysis. First, the FFT is applied to v_p and i_p, and the result is presented in Fig. 6. Since shunt current is applied to this example, the current magnitudes are equal for all injected frequencies, while the voltage amplitudes and angles depend on the system. The apparent impedance is defined in (1) as the ratio between v_p and i_p in the frequency domain.

The resulting impedance curves are presented in Fig. 7 for intersection A and in Fig. 8 for intersection B. The intersections are defined in Fig. 4. The impedances are estimated for the 8 frequencies in f_{inj}, while the Vector Fitting algorithm is used to interpolate between them. Only the impedance magnitudes are presented, but it has been verified that the angles are consistent with the conclusions. $Z_{a,shunt}$ is obtained from shunt current injection, while $Z_{a,series}$ is obtained from series voltage injection. The subsystem impedances Z_1 and Z_2 defined in Fig. 1 are also presented in the same plot. They are corresponding to the left (Buck) and right (CPL) subsystem impedances in Fig. 4, respectively. Z_1 and Z_2 are the basis for establishing the Nyquist plots in Fig. 10.

The impedance curves can be explained as follows: It is clear that the simulated apparent impedance $Z_{a,shunt}$ complies with (2) at both intersections. It represents the parallel connection of the subsystem impedances Z_1 and Z_2. When the two subsystem impedances have large difference in magnitude, $Z_{a,shunt} \approx min[Z_1, Z_2]$. A resonance peak occurs at $f_{max} = 45\ Hz$ where Z_1 and Z_2 have equal amplitude but opposite phase. At low frequencies, $Z_{a,shunt} \approx Z_1$ since

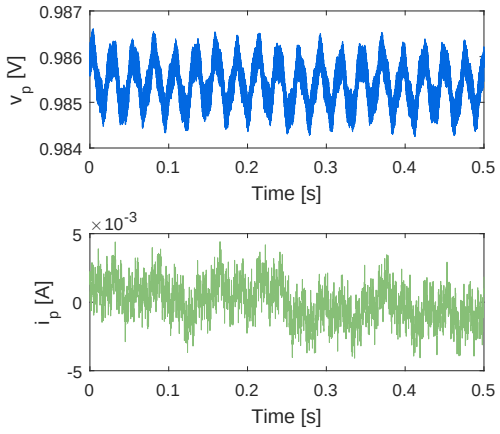

Fig. 5: Steady-state waveforms of i_p and v_p for shunt current injection at interface B. Injection frequencies given by (14)

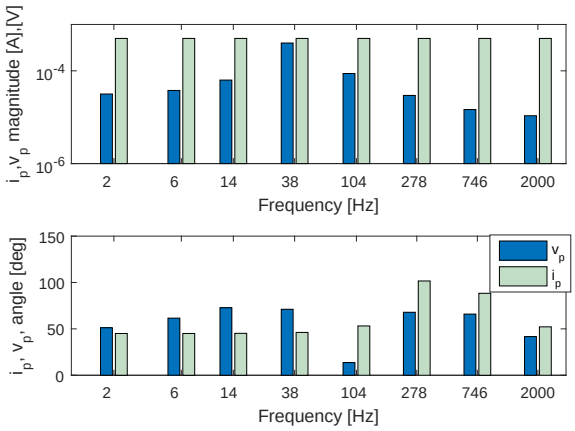

Fig. 6: Harmonic components of i_p and v_p with shunt current injection at f_{inj} (14). Obtained by FFT applied to Fig. 5

the inductive path through the buck converter has significantly lower impedance than the capacitive path through the CPL.

The simulated apparent series impedance $Z_{a,series}$ complies with (3) as the series connection of Z_1 and Z_2. When the two subsystem impedances have large difference in magnitude, $Z_{a,series} \approx max[Z_1, Z_2]$. There is also a resonant frequency at $f_{min} = 45\ Hz$ at both intersections. This is expected since the two subsystems have similar magnitude and opposite phase at this frequency.

C. Eigenvalue comparison

The next and final step in the stability analysis is to apply Vector Fitting (VF) to estimate the system state-space model, and to evaluate the eigenvalues of the matrix A. The input to VF is the set of simulated values for $Z_{a,shunt}$ or $Y_{a,series}$, along with the frequency vector f_{inj} (14).

The VF directly outputs the state-space model and eigenvalues based on the sampled values of apparent impedance/admittance. The estimated (apparent) eigenvalues corresponding to shunt and series injection are presented in

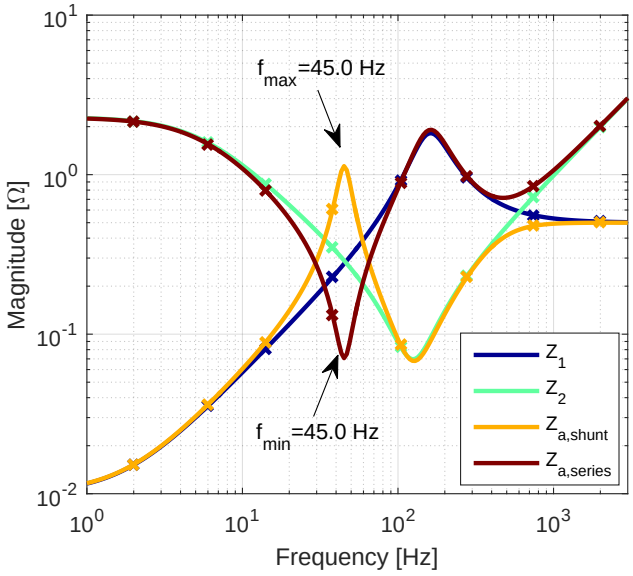

Fig. 7: Impedance curves obtained from *intersection A*. 'x' represents the simulated values at f_{inj} (14), while the solid lines represent interpolation by Vector Fitting

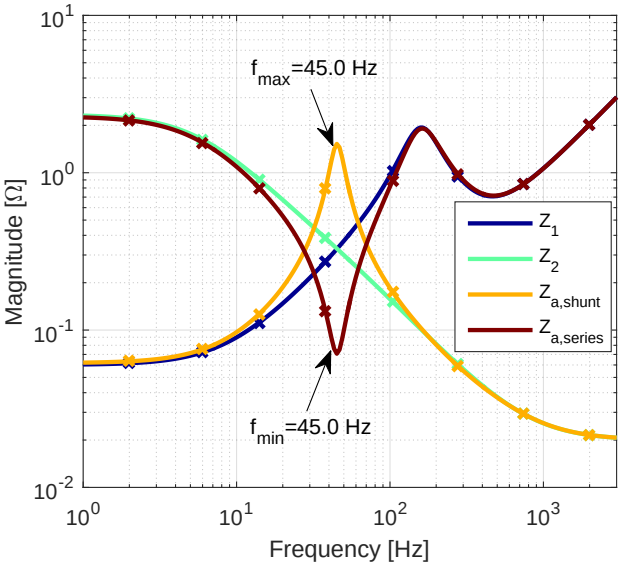

Fig. 8: Impedance curves obtained from *intersection B*. 'x' represents the simulated values at f_{inj} (14), while the solid lines represent interpolation by Vector Fitting

Table II for intersection A, and in Table III for intersection B. The difference between apparent eigenvalues and the analytical ones is less than 0.01 % at both intersections. The eigenvalues are visualized in a plot in Fig. 9. The most critical eigenvalue has an imaginary part equal to 282.8, which is equivalent to an oscillation frequency of $\frac{282.8}{2\pi} = 45.0\ Hz$. This is the same frequency as the apparent impedance resonances in Fig. 7 and 8. It is also the oscillation frequency identified in Fig. 11.

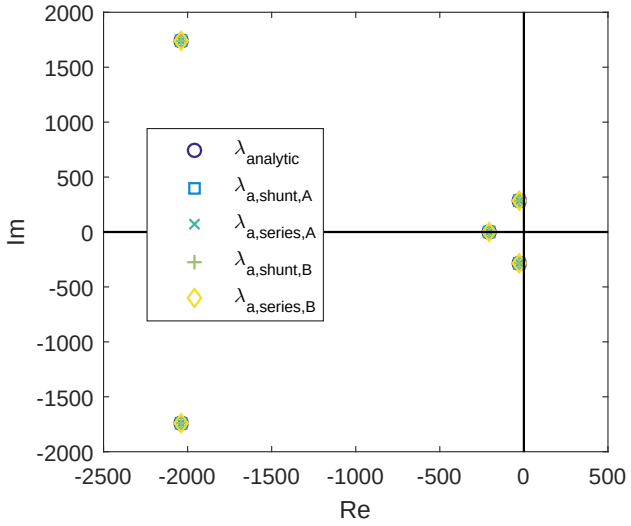

Fig. 9: Comparison of analytical and apparent eigenvalues in Table II and III at both interfaces

TABLE II: Comparison of analytical eigenvalues with the apparent eigenvalues obtained at intersection A

$\lambda_{analytic}$	$\lambda_{a,shunt,A}$	$\lambda_{a,series,A}$
$-30.39 \pm j282.8$	$-30.37 \pm j282.6$	$-30.37 \pm j282.6$
$-2039.3 \pm j1742.8$	$-2039.3 \pm j1742.7$	$-2039.3 \pm j1742.7$
-208.7	-208.7	-208.8

TABLE III: Comparison of analytical eigenvalues with the apparent eigenvalues obtained at intersection B

$\lambda_{analytic}$	$\lambda_{a,shunt,B}$	$\lambda_{a,series,B}$
$-30.39 \pm j282.8$	$-30.37 \pm j282.6$	$-30.37 \pm j282.6$
$-2039.3 \pm j1742.8$	$-2039.3 \pm j1742.5$	$-2039.3 \pm j1742.7$
-208.7	-208.8	-208.8

D. Nyquist criterion analysis

It has been stated in the introduction that the traditional impedance-based stability analysis will give a result dependent on the measurement location. This has been investigated by applying the Nyquist Criterion to the ratio $L = \frac{Z_1}{Z_2}$ at both intersections A and B (11). Z_1 and Z_2 are the subsystem impedances plotted in Fig. 7 and 8. Z_1 represents the source subsystem (Buck converter), while Z_2 is the load (CPL).

The Nyquist curves are plotted in Fig. 10. The lower figure is a close-up showing the behavior in proximity of the unit circle. It is clear from the figure that neither of the Nyquist curves encircle the critical point $(-1, 0)$, but the trajectories are different. The curve at intersection A crosses the unity circle twice, while intersection B only once. This is corresponding to the fact that Z_1 and Z_2 have equal magnitude at two frequencies for intersection A (Fig. 7), but only for one frequency at interface B (Fig. 8). The frequency corresponding to the most critical unity circle crossing is 45.9 and 45.1 Hz for intersection A and B, respectively. This is very close to the imaginary part of the most critical eigenvalue, and also to the resonance points of the apparent impedance.

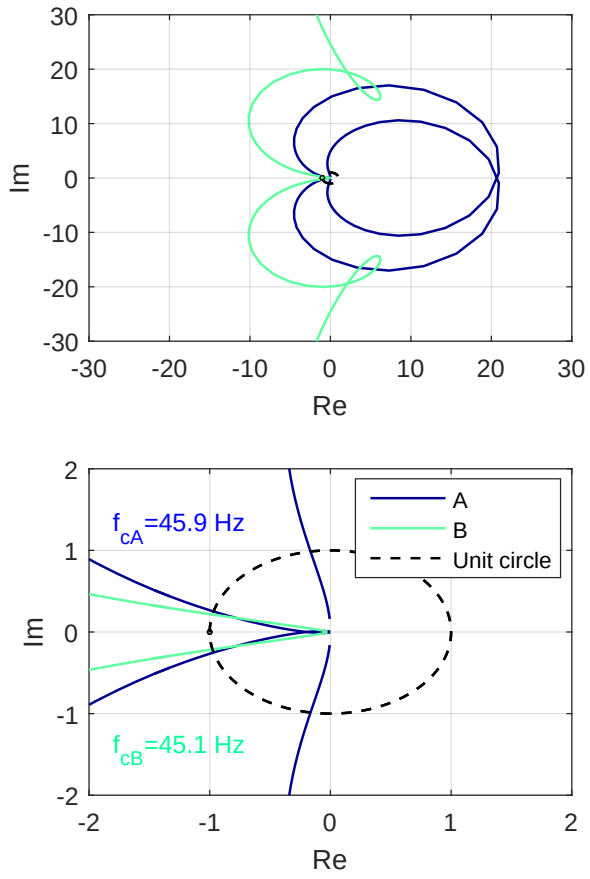

Fig. 10: Nyquist plots evaluated at both intersections

Although the Nyquist plot differences are not significant in the specific case study, it can be concluded that the Nyquist criterion gives a local stability margin dependent on the measurement location. By contrast, the apparent impedance method gives a global stability margin since the system eigenvalues are estimated.

E. Transient response example

To illustrate the relation between the impedance analysis and time-domain responses, an example simulation is presented in Fig. 11. Initially the system operates according to the parameters in Table I. At $t = 0$ the reference CPL power is increased with 10 % to $P^* = 0.55$ W. The disturbance injection has been disabled during this simulation. The transient response of the voltage v_{C2} and the line current i_{L2} are plotted. An oscillatory mode is triggered during the step, and the frequency has been accurately estimated as $f = 44.8$ Hz by zooming into the plot. This is very close to the frequency predicted by the apparent impedance, by the eigenvalues, and also by the Nyquist plots. A small deviation from 45.0 Hz can be explained from the fact that the operation point is slightly shifted during this step, which will affect the non-linear part of the system.

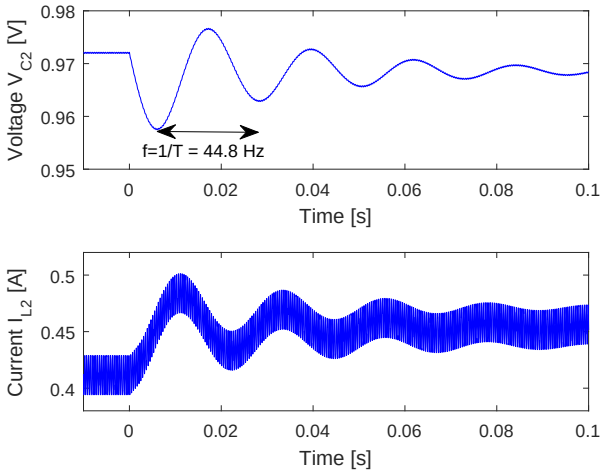

Fig. 11: Response of v_{C2} and i_{L2} to 10 % step increase in P^*

VI. Conclusions

The apparent impedance stability analysis method has been defined in this paper along with an example case study. The method has been defined for DC-system, while further work will extend the theory to single-phase and three-phase AC systems. It has been shown that the apparent impedance can be used to estimate the eigenvalues of the system that are observable from the injection point. The eigenvalues are directly obtained by applying the Vector Fitting algorithm to the measured set of apparent impedances. The proposed method holds some advantages over the well established impedance-based analysis method: It is no longer needed to estimate the source and load impedance equivalents, and it is not necessary to make any assumption regarding where the source and load are located.

In the case study it was found that there are three methods for estimating the dominant oscillatory mode of the system:

- Resonance points in the apparent impedance
- Imaginary part of most critical eigenvalue
- Frequency of Nyquist curve unity circle crossing

Further work should analyze the robustness of the apparent impedance method compared with the well established source/load impedance method. The requirements related with observability should be explored in detail. Finally, it is remarked that sensitivity to noise and measurement errors are critical aspects for experimental implementation.

References

[1] R. D. Middlebrook, "Input filter considerations in design and application of switching regulators," in *IEEE Industry Applications Society Annual Meeting*, 1976.

[2] M. Belkhayat, *Stability criteria for AC power systems with regulated loads*. Purdue University, 1997.

[3] J. Sun, "Small-signal methods for ac distributed power systems;a review," *Power Electronics, IEEE Transactions on*, vol. 24, no. 11, pp. 2545–2554, Nov 2009.

[4] B. Gustavsen and A. Semlyen, "Rational approximation of frequency domain responses by vector fitting," *Power Delivery, IEEE Transactions on*, vol. 14, no. 3, pp. 1052–1061, Jul 1999.

[5] B. Gustavsen, "Improving the pole relocating properties of vector fitting," *Power Delivery, IEEE Transactions on*, vol. 21, no. 3, pp. 1587–1592, July 2006.

[6] D. Deschrijver, M. Mrozowski, T. Dhaene, and D. De Zutter, "Macromodeling of multiport systems using a fast implementation of the vector fitting method," *Microwave and Wireless Components Letters, IEEE*, vol. 18, no. 6, pp. 383–385, June 2008.

[7] "The vector fitting web page," https://www.sintef.no/projectweb/vectfit/, accessed: 2016-02-19.